

Review: Advances in delta-subsidence research using satellite methods

Stephanie A. Higgins^{1,2,3}

Received: 16 March 2015 / Accepted: 19 October 2015
© Springer-Verlag Berlin Heidelberg 2015

Abstract Most of the world's major river deltas are sinking relative to local sea level. The effects of subsidence can include aquifer salinization, infrastructure damage, increased vulnerability to flooding and storm surges, and permanent inundation of low-lying land. Consequently, determining the relative importance of natural vs. anthropogenic pressures in driving delta subsidence is a topic of ongoing research. This article presents a review of knowledge with respect to delta surface-elevation loss. The field is rapidly advancing due to applications of space-based techniques: InSAR (interferometric synthetic aperture radar), GPS (global positioning system), and satellite ocean altimetry. These techniques have shed new light on a variety of subsidence processes, including tectonics, isostatic adjustment, and the spatial and temporal variability of sediment compaction. They also confirm that subsidence associated with fluid extraction can outpace sea-level rise by up to two orders of magnitude, resulting in effective sea-level rise that is one-hundred times faster than the global average rate. In coming years, space-based and airborne instruments will be critical in providing near-real-time monitoring to facilitate management decisions in sinking deltas. However, ground-based observations continue to be necessary for generating complete measurements of surface-elevation change.

Published in the theme issue "Land Subsidence Processes"

✉ Stephanie A. Higgins
stephanie.higgins@colorado.edu

¹ Department of Geological Sciences, University of Colorado Boulder, Boulder, CO, USA

² Institute of Arctic and Alpine Research, University of Colorado Boulder, UCB 450, Boulder, CO 80301-0450, USA

³ Community Surface Dynamics Modeling System (CSDMS), University of Colorado Boulder, Boulder, CO, USA

Numerical modeling should seek to simulate couplings between subsidence processes for greater predictive power.

Keywords Review · Geohazards · Subsidence · Groundwater extraction · Relative sea-level rise

Introduction

Modern river deltas began to form 6,500 to 8,500 years ago, as sea level stabilized following the end of the last glacial period. Lush vegetation, organic-rich soils and freshwater distributary channels quickly drew humans to settle in deltaic areas (Stanley and Warne 1997). Today, more than 600 million people live on or near river deltas, where the productive intersection of river and ocean has allowed port cities to flourish: Bangkok (Thailand), Yangon (Myanmar), Shanghai (China), Hong Kong (China), Dhaka (Bangladesh), New Orleans (USA), Ho Chi Minh City (Vietnam), and many others. Outside of the cities lie vast agricultural and aquacultural operations that have earned deltas—particularly Asian megadeltas—the nickname “rice bowls of the world.” Deltas are also home to innumerable wetlands, mangrove forests and ecological reserves. Taken together, these resources make river deltas some of the most important economic and environmental areas on Earth.

The fluvial origin of deltas has long been understood. Herodotus wrote of the Nile Delta in *The Histories*: “But the delta, as the Egyptians affirm, and as I myself am persuaded, is formed of the deposits of the river” (Herodotus 440 BC). Herodotus also understood that these deposits were carried in annual floods that slowly increased land elevation. Deltas are transient landforms by nature, characterized in their pristine state by ever-changing waterways and shifting sediment carried by storms and floods. New sediment compensates for

regional subsidence and the compaction of older sediment, resulting in a prograding landform that builds into the sea.

After thousands of years of progradation, that balance has shifted. Most major river deltas are now sinking relative to local sea level (Ericson et al. 2006; Woodroffe et al. 2006; Syvitski et al. 2009). Figure 1 shows the world's largest and most populous deltas – those with land areas greater than 10,000 km², populations greater than 1 million, or both. Values are given in Tables 1 and 2. More than half of these deltas are losing elevation with respect to the sea—the Mississippi (USA), Rio Grande (USA/Mexico), Magdalena (Colombia), Parana (Argentina), Niger (Nigeria), Nile (Egypt), Godavari (India), Mahanadi (India), Brahmani (India), Ganges-Brahmaputra (India/Bangladesh), Irrawaddy (Myanmar), Chao Phraya (Thailand), Mekong (Vietnam), Pearl (China), Yangtze (China), and Yellow (China)—as are numerous smaller deltas in North America, Europe and Asia (Syvitski et al. 2009; and Stanley and Randazzo 2001 for the Rio Grande).

A portion of this elevation loss is attributable to sea-level rise, which is proceeding at a global average of 3.3 ± 0.4 mm/year and is expected to accelerate in the coming century (Church et al. 2013). Satellite ocean altimetry shows that some parts of the ocean are experiencing local sea-level rise of up to 10 mm/year, primarily due to variations in surface heating (Milne et al. 2009; Nicholls and Cazenave 2010). In many deltas, however, natural processes and anthropogenic pressures are driving additional subsidence of the land itself. Extraction of groundwater, oil and gas has resulted in meters of subsidence in some deltas. Sediment trapping by dams and reservoirs, reduced river flows and widespread loss of coastal

Table 1 Deltas with populations greater than one million people. Locations are given in Fig. 1. Population data is from Center for International Earth Science Information Network 2.5 Arc-Minute Gridded Population of The World ver. 3 future estimates for 2015 (CIESIN 2005). Delta boundaries are from the subset defined by Tessler et al. (2015)

| Name | 2015 population (10 ⁶) |
|-------------|------------------------------------|
| Grijalva | 1.20 |
| Rhine | 1.89 |
| Rio Grande | 1.90 |
| Mississippi | 1.96 |
| Magdalena | 2.00 |
| Godavari | 2.59 |
| Han | 2.83 |
| Brahmani | 3.39 |
| Amazon | 3.69 |
| Niger | 4.57 |
| Mahanadi | 4.70 |
| Yellow | 5.79 |
| Hong | 6.44 |
| Irrawaddy | 11.7 |
| Chao Phraya | 18.6 |
| Mekong | 24.7 |
| Pearl | 25.8 |
| Yangtze | 38.9 |
| Nile | 49.9 |
| Ganges | 144.1 |

vegetation are hastening deltas' decay. Subsidence increases a delta's vulnerability to flooding and, in extreme cases,

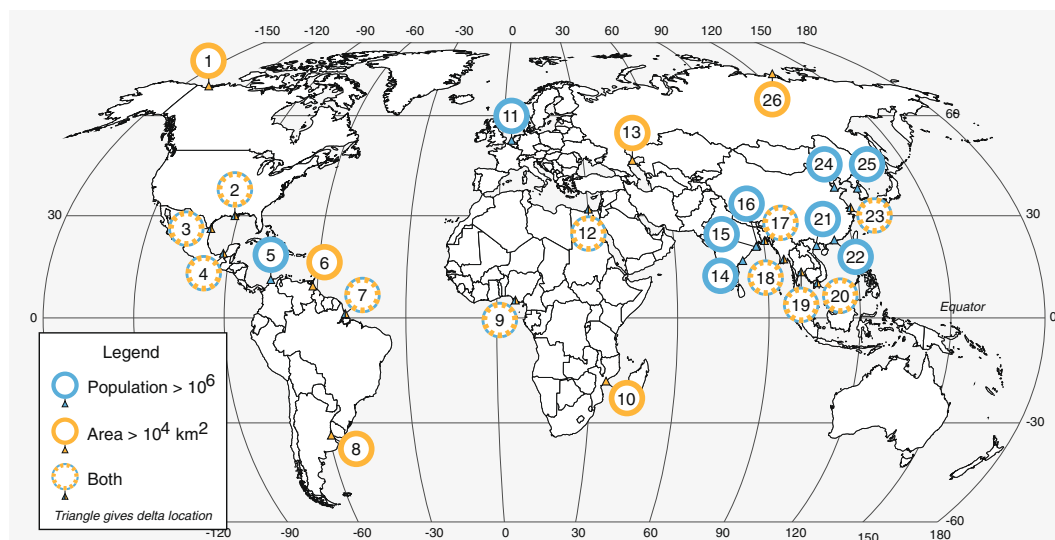


Fig. 1 Locations of the world's largest and most populous deltas: those with 2015 populations greater than one million, land areas greater than 10,000 km², or both. Population and area values are given in Tables 1 and 2. (1) Mackenzie, (2) Mississippi, (3) Rio Grande, (4) Grijalva, (5) Magdalena, (6) Orinoco, (7) Amazon, (8) Parana, (9) Niger, (10)

Zambezi, (11) Rhine, (12) Nile, (13) Volga, (14) Godavari, (15) Mahanadi, (16) Brahmani, (17) Ganges-Brahmaputra, (18) Irrawaddy, (19) Chao Phraya, (20) Mekong, (21) Hong, (22) Pearl, (23) Yangtze, (24) Yellow, (25) Han, (26) Lena

Table 2 Deltas with areas greater than 10,000 km². Locations are given in Fig. 1. Delta boundaries are from the subset defined by Tessler et al. (2015)

| Name | Area (10 ³ km ²) |
|-------------|---|
| Volga | 10.3 |
| Grijalva | 10.4 |
| Zambezi | 11.2 |
| Parana | 12.9 |
| Mackenzie | 13.8 |
| Rio Grande | 13.9 |
| Niger | 17.6 |
| Chao Phraya | 20.8 |
| Lena | 21.1 |
| Nile | 24.9 |
| Orinoco | 25.5 |
| Mississippi | 30.7 |
| Irrawaddy | 30.7 |
| Yangtze | 34.0 |
| Mekong | 48.9 |
| Ganges | 88.1 |
| Amazon | 106.0 |

necessitates the construction and long-term maintenance of protective infrastructure. Future changes to the costs of building and maintaining such infrastructure due to, for example, increased energy prices, higher labor costs, or rising interest rates, could alter decision-making and increase risk in countries with higher GDPs (Tessler et al. 2015).

This article presents a review of knowledge with respect to delta surface elevation loss. The processes that drive subsidence include tectonics, isostatic adjustment, natural sediment compaction, peat oxidation, accelerated compaction due to fluid extraction, reduced aggradation and the loss of coastal vegetation. Our ability to map the consequent subsidence is rapidly advancing due to applications of space-based techniques: InSAR (interferometric synthetic aperture radar), GPS (Global Positioning System), and satellite ocean altimetry. These same techniques will be critical in providing near-real-time monitoring to facilitate management decisions in sinking deltas.

A global problem

Subsidence in individual deltas has been recognized for hundreds of years. In the Rhine Delta in the Netherlands, regional water boards were organized as early as the 1300s to manage drainage and flood control in the lowlands (TeBrake 2002). In Shanghai (Yangtze River Delta), subsidence due to groundwater extraction has been monitored by government officials since 1921 (Xu et al. 2008). It was not until the 21st century, however, that subsidence came to be seen as a widespread phenomenon characteristic of deltas. In 2006, a literature

review of nine Asian megadeltas found that the Chao Phraya, Ganges, Red, Pearl, Yangtze and Yellow River deltas were all experiencing subsidence, with the remaining three megadeltas (the Indus, Irrawaddy and Mekong) potentially experiencing subsidence but at unknown rates (Woodroffe et al. 2006). Ericson et al. (2006) modeled relative sea level rise at 40 river deltas, assuming uniform global sea-level rise of 3.5 mm/year and estimating sediment reduction by evaluating upstream reservoir trapping and water withdrawals. Results showed that, by the year 2050, the Godavari, Mississippi, Orinoco (Venezuela) and Sao Francisco (Brazil) deltas could experience greater than 10 % land loss due to flooding, and the Ganges-Brahmaputra, Mekong, Mississippi, Nile and Yangtze deltas will host more than 400,000 people affected by subsidence.

It was a space-based technique that first allowed the global extent of delta subsidence to be quantified. In February 2000, the Shuttle Radar Topography Mission (SRTM) collected elevation measurements over most of the Earth at a spatial resolution of 90 m or less. Syvitski et al. (2009) analyzed SRTM digital elevation models (DEMs) for 33 major river deltas, a selection of which are shown in Fig. 2. Shades of pink indicate land that was already below sea level in the year 2000. In total, Syvitski et al. (2009) found that more than 26,000 km² of delta land had fallen below sea level worldwide. Moreover, Syvitski et al. (2009) examined aggradation rates and compared them with published tide gauge records and DEMs in order to determine the risk of future delta inundation. The authors concluded that the Ganges-Brahmaputra, Irrawaddy, Magdalena, Mekong, Mississippi, Niger, and Tigris (Iraq/Iran) deltas are sinking faster than sea level is rising, and the Chao Phraya, Colorado (USA), Krishna (India), Nile, Pearl, Po (Italy), Rhone (France), Sao Francisco, Tone (Japan), Yangtze and Yellow River deltas have virtually no aggradation and/or are subject to heavy oil and gas extraction that places them in great peril of flooding and inundation.

In addition to these global surveys, myriad studies have been conducted on individual deltas in order to investigate potential drivers of subsidence. The following sections review current progress towards understanding the magnitude, spatial variability and temporal variability of subsidence drivers in river deltas.

The delta balance

Deep processes

There are several deep processes that affect relative sea level at river deltas. First, many deltas are located in subsiding basins that created the accommodation space required for their continuous growth throughout the Holocene. Tectonic motion in these basins can be broad or localized and perhaps episodic;

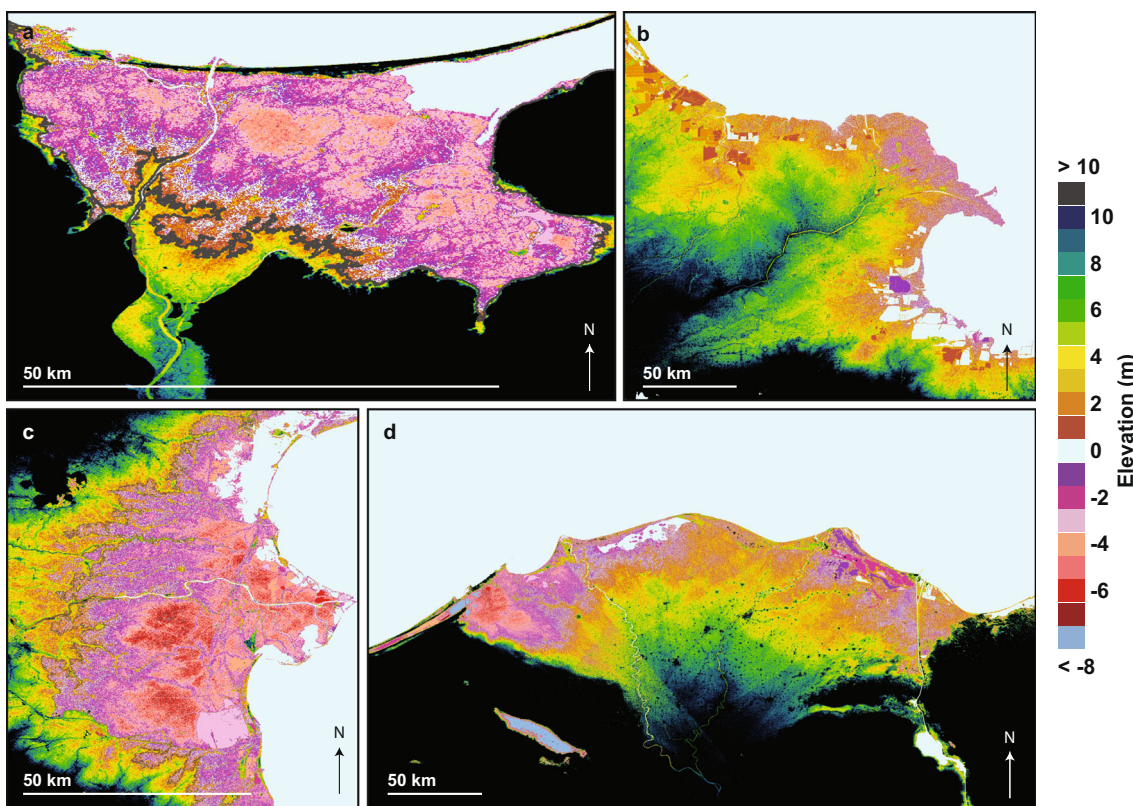


Fig. 2 Delta surface elevations from Syvitski et al. (2009), produced from Shuttle Radar Topography Mission (SRTM) data collected in the year 2000. **a** Vistula Delta, Poland; **b** Yellow River (Huanghe) Delta, China; **c** Po Delta, Italy; **d** Nile River Delta, Egypt. Elevations greater

than 10 m are masked. *Shades of pink* show elevations that are below sea level. Adapted by permission from Macmillan Publishers Ltd: Nature Geoscience 2: 681–686, 2009

Goodbred et al. (2003) argues that the Ganges-Brahmaputra Delta is partitioned into sub-basins that control channel motion and the retention of sediment. In the Mississippi River Delta, leveling surveys measured 16.9 mm/year of subsidence associated with motion along the Michoud Fault between 1969 and 1971, and 7.1 mm/year of subsidence at the same location between 1977 and 1995 (Dokka 2006). Splays of the Red River Fault Zone are exposed on land in the Red River Delta, and the faults were an important control on the delta's development in the past (Rangin et al. 1995).

Isostatic adjustment is the viscoelastic response of the Earth's crust under a change in the weight of overlying material such as water, sediment or ice. Glacial isostatic adjustment (GIA) refers specifically to the response associated with the melting of glaciers and ice sheets. After the end of the last glacial period, melting was complete by ~6 ka, but much of northern Europe continues to rise by up to 1 cm/year (Johansson et al. 2002). This can be seen in tide gauge records that record falling sea level in the region (Emery and Aubrey 1985). Moreover, mantle material flowing from under the ocean toward the rebounding crust both exerts a gravitational pull on the ocean and increases the ocean basin volume. Rotational changes associated with the redistribution of ice and mantle material also contribute to GIA. When all of these

factors are accounted for, the average rate of relative sea level change from 6 ka to the present is thought to be small (<1 mm/year) outside of Canada and northern Europe (Peltier 1999; Milne and Mitrovica 2008), but the effect can be large in previously glaciated areas or when longer time-scales are considered. Delta regions can also respond isostatically to the weight of the delta itself. Using numerical modeling, Ivins et al. (2007) demonstrate that sediment loading can cause up to 8 mm/year of subsidence in a deltaic region. Similarly, as sea level rises, continental shelves steepen in response to the weight of the overlying sea water (Jouet et al. 2008; Hutton et al. 2013).

Large deltas can deform elastically on annual time-scales, a phenomenon that has been observed by arrays of GPS devices in the Ganges-Brahmaputra Delta. These instruments show that the entire delta undergoes vertical elastic deformation of up to 6 cm each year due to annual loading and unloading of surface water and groundwater and the response of the underlying lithosphere (Steckler et al. 2010). The mass of the impounded water can be estimated using observations from the Gravity Recovery and Climate Experiment (GRACE) satellite (Steckler et al. 2010). The mean annual discharge of the Ganges-Brahmaputra-Meghna system is the second largest in the world, and terrestrial water storage in the delta is unusually

high; whether this phenomenon occurs in other deltas is a topic of ongoing research.

Reduced aggradation

Aggradation is an increase in surface elevation due to sediment deposition. It can happen slowly and steadily through annual river floods, or in large events such as storm surges. The shoreline of a natural river delta is determined by a balance between aggradation, sediment compaction, regional land motion, and sea level. When sea level and sediment supply are constant, natural deltas generally maintain a stable location with respect to the sea (Sanchez-Arcilla et al. 1998; Syvitski et al. 2009).

At first, human activities tend to increase the amount of sediment entering rivers. Agriculture, mining, and deforestation can cause substantial erosion; for example, sediment loads in the Yellow, Po, and Mississippi rivers more than doubled after humans occupied the watersheds (McManus 2002; Syvitski 2008). Human activities in the Ebro watershed over the last 4,000 years caused an estimated sediment load increase of 17 Mt/year, potentially contributing substantially to deltaic growth (Xing et al. 2014). Increased sediment load does not always translate to increased deposition at the delta, however. As countries industrialize, artificial dams and reservoirs are constructed that trap sediment upstream, reducing sediment discharge dramatically. Syvitski and Kettner (2011) document the rate of dam construction in the United States over the last 150 years: prior to 1800, there were no dams higher than 15 m in the United States, while there are more than 8,000 large dams today. In Spain, the 170 dams that cross the Ebro River have reduced its sediment load to less than 1 % of the pre-1960 value (Ibanez et al. 1996). Thus, the trend when humans occupy watersheds is for deltas to first see an increase in sediment, and then to receive less sediment over time (Walling and Fang 2003).

When humans occupy the delta itself, anthropogenic modifications typically control the flow of water and sediment. The Nile Delta in Egypt saw the construction of substantial irrigation projects beginning more than 2,000 years ago (Stanley and Warne 1993), and construction of the first major diversion of the Po River in Italy began as early as AD 1150 (Syvitski et al. 2005). In the Netherlands, written references from the 11th century describe dikes in the Rhine-Meuse Delta (Wolff 1992). Levees, canals, and sluice gates have had great benefits, increasing agricultural productivity, facilitating transport, and offering protection from floods. Unfortunately, they also prevent sedimentation, disrupting the balance that preserves surface elevation in natural deltas.

Engineers and policy-makers have long recognized the trade-offs involved in embanking a delta. R. R. Twilley and colleagues at Louisiana State University examined the case of the Mississippi River Delta, where the decision to embank

was made with the full knowledge that levees would cause a net loss of elevation and perhaps the permanent loss of land. The authors point to an 1897 article in *National Geographic*, which argues: “No doubt the great benefit to the present and two or three following generations accruing from a complete system of absolutely protective levees, excluding the flood waters entirely from the great areas of the lower delta country, far outweighs the disadvantages to future generations from the subsidence of the Gulf delta lands below the level of the sea and their gradual abandonment due to this cause” (Corthell 1897).

Floodplains are frequently narrowed or eliminated by development of the land adjacent to the levees. Sediment deposition is then restricted to the area between the walls of the embankment. This can cause the floors of the distributary channels to become super-elevated while the rest of the delta subsides. The distributary channel beds of the Po Delta, for example, aggrade at rates of up to 100 mm/year with respect to the surrounding land (Syvitski et al. 2005). Levees also alter natural aggradation patterns by preventing distributary channels from avulsing. In a natural delta, distributary channels are constantly changing course as the delta-plain gradient undergoes small local changes. Anthropogenic influence tends to reduce the number of distributary channels on deltas; the number of distributary channels in the Po Delta has decreased from 16 to 6 in the last century, and in the Nile Delta the number of channels has decreased from 15 to 6 (Syvitski and Saito 2007).

Humans also modify sediment fluxes by reducing streamflow. Globally, humans reroute and use more than half of the renewable water supply (Vorosmarty and Sahagian 2000). This reduces a stream’s ability to transport sediment, causing sedimentation to happen upstream rather than at the river mouth. The Yellow (Huanghe) riverbed, for example, is 10 m above the surrounding land (Shu and Finlayson 1992) and must be scoured on an annual basis with massive water releases from the Xiaolangdi Reservoir. These releases occur for 10–20 days each summer and account for 30–45 % of the river’s annual sediment discharge and 15–60 % of its annual water discharge, both of which are less than 15 % of their pre-1950s levels (Wang et al. 2010). Sediment transported by high discharge events also tends to be of a larger grain size than sediment transported by regular river floods, affecting organisms adapted to the smaller grain size (Wang et al. 2010; Rogers et al. 2013a).

Vegetation can play a critical role in trapping and retaining sediment. Numerous saltmarshes in the United States have collapsed due to biological disturbances such as fungal pathogens or grazing snow geese that destroy *Spartina alterniflora* or *S. patens*, the two primary grasses in estuarine saltmarshes (Alber et al. 2008; Fig. 3). In the Bayou Chitigne of the Mississippi River Delta, for example, a sudden small decrease in surface elevation doubled the days per year that the marsh



Fig. 3 *Spartina alterniflora* and *S. patens* zonation in a New England salt marsh. *S. alterniflora* (the taller grass) has been shown to be less effective than *S. patens* (the shorter grass) at trapping and retaining sediment (Warren and Niering 1993), but disturbances to either species can reduce aggradation (Cahoon et al. 2004; Day et al. 2011). Photo credit: Tyler Coverdale, Princeton University, used with permission

spent underwater. Marsh grass in the bayou died due to the resultant waterlogging (Day et al. 2011). Without vegetation, sediment was not effectively retained, and the marsh collapsed within fifteen years despite an ample supply of sediment in the regular floodwaters. The Old Oyster Bayou received 30 % less net sediment flux and 60 % less short-term deposition than Bayou Chitigue during the same period, but its healthy vegetation allowed long-term retention that kept the marsh aggrading (Day et al. 2011). Mangrove forests are similarly complex; mangroves with prop roots are more successful at capturing sediment in the short-term, while those with aerial roots bolster soil elevation and aid sediment retention in the long-term (Krauss et al. 2003). Small changes in a mangrove forest community can change or even halt aggradation rates. This is worrisome given that more than 20 % of the world's mangrove forests—3.6 million ha—were lost between 1980 and 2005 (FAO 2007).

Aggradation is strongly affected by both natural environmental changes and human activities. It is also likely that aggradation is coupled to other subsidence drivers. For example, fault slip may change the height of part of a delta, rerouting distributary channels and changing local aggradation rates. The new weight distribution might then affect the internal stresses in the delta. Aggradation rates are typically millimeters to centimeters per year, but rates vary widely between and within deltas. It is not yet well known whether regular river flooding or major storm events cause more deposition; simulating these events and tracking grain size with numerical models is a logical next step in delta elevation research.

Root bulking and peat formation

In addition to trapping and retaining sediment, vegetation can contribute directly to surface elevation through root bulking. When vegetation is healthy, root production can contribute to surface elevation gains. Cahoon et al. (2006) measured

vertical soil expansion in 30 mangrove forests with varying soil types (mineral, organic and peat). Root volume increases contributed to vertical expansion in 26 of the 30 mangrove forests, at rates of 1–3 mm/year (Cahoon et al. 2006). Conversely, when vegetation dies, roots may rot underground, causing subsidence of several centimeters (Cahoon et al. 2003, 2004; Day et al. 2011).

Vegetation also contributes to delta surface elevation by depositing organic detritus (plant litter). In saturated soil, this detritus accumulates to form peat. Allen (1990) showed that the rate of production of organic material determines the marsh type—minerogenic or organogenic—in a pristine delta. Where organic detritus is produced more quickly than sea level rises, peat marshes form. Peat can accumulate at rates of several centimeters per year; in the Klang-Langat Delta in Malaysia, for example, peat accumulates at ~10 mm/year (Coleman 1969), and in the Okavango Delta in Botswana (an inland delta), peat accumulation rates are as high as 40 mm/year, though fires destroy much of the accumulated material (McCarthy et al. 1988).

When peat is saturated, decomposition of organic material within the soil proceeds anaerobically, and new material accumulates more quickly than it decays. When peat is drained, however, decomposition is much more efficient. Peat that has been drained for agriculture or other purposes can decompose up to 100 times faster than new material can accumulate, at rates that approach 100 mm/year (Galloway et al. 1999). The decomposition of drained peat occurs due to a combination of biological and chemical processes that are often collectively referred to as “oxidation,” although the term is sometimes reserved only for the chemical processes of decomposition (e.g., van Asselen et al. 2009), with the term “bio-oxidation” used for both (e.g., Gambolati et al. 2005). In the Rhine Delta in the Netherlands, peat was drained for agriculture beginning as early as AD 1000. Oxidation caused peat domes 3–4 m high to fall below sea level or disappear completely by the 1600s (Hoeksema 2007). In and just north of the Po Delta in Italy, farmland drained between 1892 and 1967 has experienced up to 2 m of subsidence due in part to oxidation of peat-rich histosols (Gambolati et al. 2006). The Sacramento Delta, a vital agricultural area and freshwater source for two-thirds of Californians, lies 3 to 7 m below sea level due to peat drainage that began in the 1860s (Ingebritsen and Ikehara 1999). In modern-day Indonesia, 12.9 million ha of peatland have been deforested, drained, and sometimes burned to make way for oil palm and pulpwood plantations, resulting in several meters of land subsidence as well as up to 855 Mt/year of carbon dioxide emissions (Hooijer et al. 2010).

Natural compaction

River deltas are built from sands, silts, clays and peats that compact naturally under their own weight. New layers exert

pressure on underlying layers, which consolidate by expelling water. In unsaturated soil, compaction occurs—an analogous process to consolidation, but involving a reduction in void space rather than a loss of pore water. Natural compaction rates depend primarily on overburden thickness and grain size. Gravel (diameter $d=2.0\text{--}64.0$ mm) and sand ($d=0.063\text{--}2.0$ mm) are nearly incompressible and lose little volume after deposition (Allen 1999). Silt ($d=0.004\text{--}0.063$ mm) is more compressible, and the porosity of newly deposited silt can drop from ~ 0.5 to ~ 0.35 within days of deposition (Shi et al. 2007). Clay ($d=0.001\text{--}0.004$ mm) is even more compressible than silt, but has a lower hydraulic conductivity, causing it to compact more slowly than silt but eventually become denser (Freeze and Cherry 1979). In a delta, a 15-m clay layer might compact 3–5 mm/year for several decades.

Peat is the most compressible soil type, and its rapid compaction has caused subsidence at many coastal locations around the world. Bloom (1964) measured peat compaction in Connecticut's coastal marshes and found that the peat had lost between 13 and 44 % of its original thickness in the 7,000 years since it was deposited. Similarly, Long et al. (2006) showed that peat compaction was a driving factor shaping the modern coastal landscape in parts of southeast England. Natural peat compaction involves compression from the weight of overlying material as well as biological and chemical processes within the peat (van Asselen et al. 2009). Natural compaction of peat typically takes place under saturated (anoxic) conditions, making it substantially slower than the anthropogenic drainage and oxidation described in the previous section.

Modeling studies confirm that natural compaction can have a significant effect on relative sea level, driving subsidence of several millimeters per year (Meckel et al. 2006, 2007; Massey et al. 2006; van Asselen et al. 2011). These rates are comparable to rates of relative sea-level rise at many of the world's deltas, and it has been suggested that natural compaction is responsible for some or all observed subsidence in some locations—e.g., Tornqvist et al. (2008) on the Mississippi River Delta.

Accelerated compaction due to fluid extraction

It has been suggested that accelerated compaction may be the dominant subsidence signal in deltas with heavy groundwater extraction (Ingebretsen and Galloway 2014). There is much evidence to support this claim. Between 1978 and 1988, groundwater pumping to supply the city of Bangkok, Thailand, caused more than 100 mm/year of subsidence in parts of the Chao Phraya Delta (Natalaya et al. 1996). From 1995 to 2005, groundwater extraction caused subsidence rates of more than 150 mm/year in Suzhou in the Yangtze River Delta (Shi et al. 2012). Recent InSAR studies confirm that subsidence due to groundwater extraction can far exceed rates

associated with any other cause. For example, subsidence of 220 mm/year associated with groundwater and gas extraction were measured in multiple Indonesian delta cities by Chaussard et al. (2013; Fig. 4). Subsidence in much of the Mekong Delta is proceeding at 10–40 mm/year due to groundwater pumping, outpacing sea-level rise by a factor of ten (Erban et al. 2014).

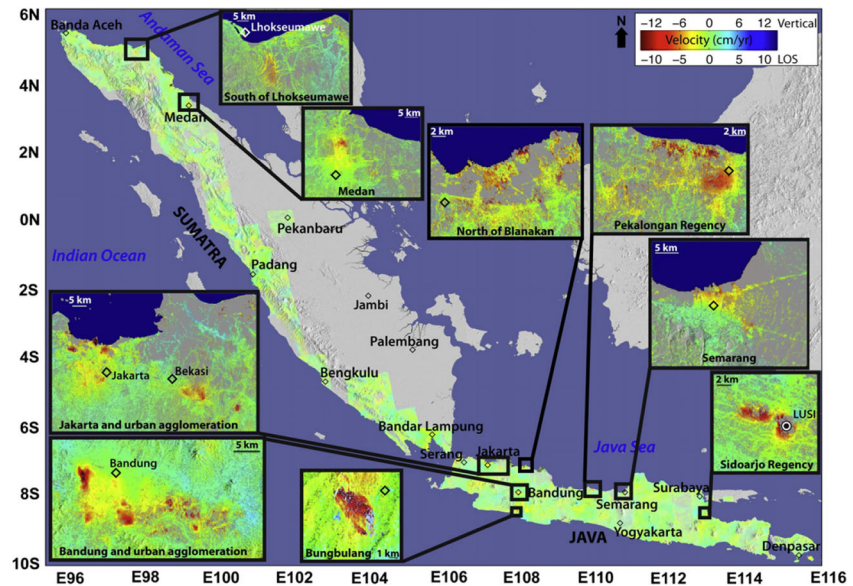
When river deltas are subject to hydrocarbon extraction, the same problems can occur. Morton and Bernier (2010) show that the decadal pattern of slow subsidence (6–7 mm/year) followed by rapid subsidence (11–12 mm/year) in the Mississippi River Delta mirrored temporal trends of hydrocarbon production in the region. On the Po Delta, relative sea level rise was 60 mm/year in 1958 (Caputo et al. 1970), but subsidence rates decreased to 12 mm/year after methane production ended (Bondesan and Simeoni 1983). Many of the world's deltas are hydrocarbon producers: Ericson et al. (2006) found that the Amazon, Yukon, Lena, Irrawaddy, Po, Rhine, Burdekin and Red (Hong) River deltas are dominated by subsidence signals from hydrocarbon extraction. Additionally, the Niger, Magdalena, Mahakam, Mackenzie, Yellow, Sacramento, and Mississippi River deltas are major hydrocarbon sources. InSAR is currently being used to monitor potential subsidence at oil fields in the Yellow River Delta (Liu et al. 2015; Zhang et al. 2015).

Though fluid extraction is well-known to drive subsidence in deltas and elsewhere, there is a dearth of data on accelerated compaction in rural areas of deltas. This is primarily for practical reasons: it can be difficult or impossible to install GPS receivers in rural or agricultural areas; leveling surveys may be infrequent; and InSAR is less commonly applied due to a lack of permanent reflectors such as buildings or roads. Nevertheless, it would be unwise to assume that substantial groundwater extraction is not occurring in rural areas of river deltas. Rural portions of deltas such as the Ganges-Brahmaputra and the Mekong are as densely populated as many United States cities ($>1,000$ people per km^2 ; CIESIN 2005). Higgins et al. (2013) observed subsidence rates of up to 250 mm/year in the Yellow River Delta, China, due to groundwater extraction at aquaculture facilities (Fig. 5). Although the area is largely rural, groundwater extraction for aquacultural and agricultural uses in the delta exceeds 1 billion m^3/year (Fan et al. 2006). It is likely that subsidence is occurring, but has not been fully quantified due to measurement difficulties. Quantifying the extent of land subsidence in rural areas should be a research priority, as agricultural and aquacultural areas are now the boundary between land and sea in much of the world.

The delta toolbox

In deltas, surface elevation change is a complex phenomenon involving many interwoven processes: crustal motion, climate

Fig. 4 Chaussard et al.'s (2013) InSAR measurements of land subsidence in Indonesia. Reprinted from Chaussard et al. (2013), Sinking cities in Indonesia: ALOS PALSAR detects rapid subsidence due to groundwater and gas extraction, *Remote Sensing of the Environment* 128:150–161, 2013, with permission from Elsevier



and runoff, vegetation dynamics, erosion, aggradation, sediment compaction, peat oxidation, and sediment transport by waves, tides, currents and storms. These processes cross traditional disciplinary boundaries, requiring methods from sedimentology, solid-earth geology, oceanography, biology, hydrology, and engineering to measure their effects. Few existing instruments can measure total elevation change, and none can resolve every process across all pertinent spatial and temporal scales. Tide gauges, extensometers, sediment cores, GPS devices and marker horizons allow point measurements of subsidence and/or sedimentation rates, while recent advances in InSAR and LiDAR allow unprecedented high-resolution mapping capacity. However, each method can resolve only certain pieces of delta surface elevation change at certain spatial and temporal resolutions. The following sections assess the advantages of limitations of each methodology, with an emphasis on the particular subsidence processes that can and cannot be resolved and the ways that techniques can be combined to generate a more complete picture of delta behavior.

Measuring sea level rise

Throughout most of the 20th century, tide gauges and leveling surveys were the primary methods for measuring relative sea level change in deltas. Tide gauge measurements are sensitive to instantaneous water level changes of $\sim 100 \mu$, but records of at least 30 years are needed before meaningful trends can be established (Douglas 2001). Tide gauges do not differentiate between sea surface elevation change and land elevation change, measuring only the difference between the two. However, the advent of satellite altimetry now allows tide gauge measurements to be differenced from sea surface elevation changes, offering a new measure of land subsidence

(e.g., Ostanciaux et al. 2012). Satellite altimetry is also unique in its capacity to offer estimates of absolute sea-level rise at individual deltas: for example, the Ganges-Brahmaputra Delta is experiencing absolute sea-level rise of 2–5 mm/year, while deltas in Indonesia see >20 mm/year, and deltas on the west coast of North America have actually seen sea level fall over the last two decades (Nicholls and Cazenave 2010).

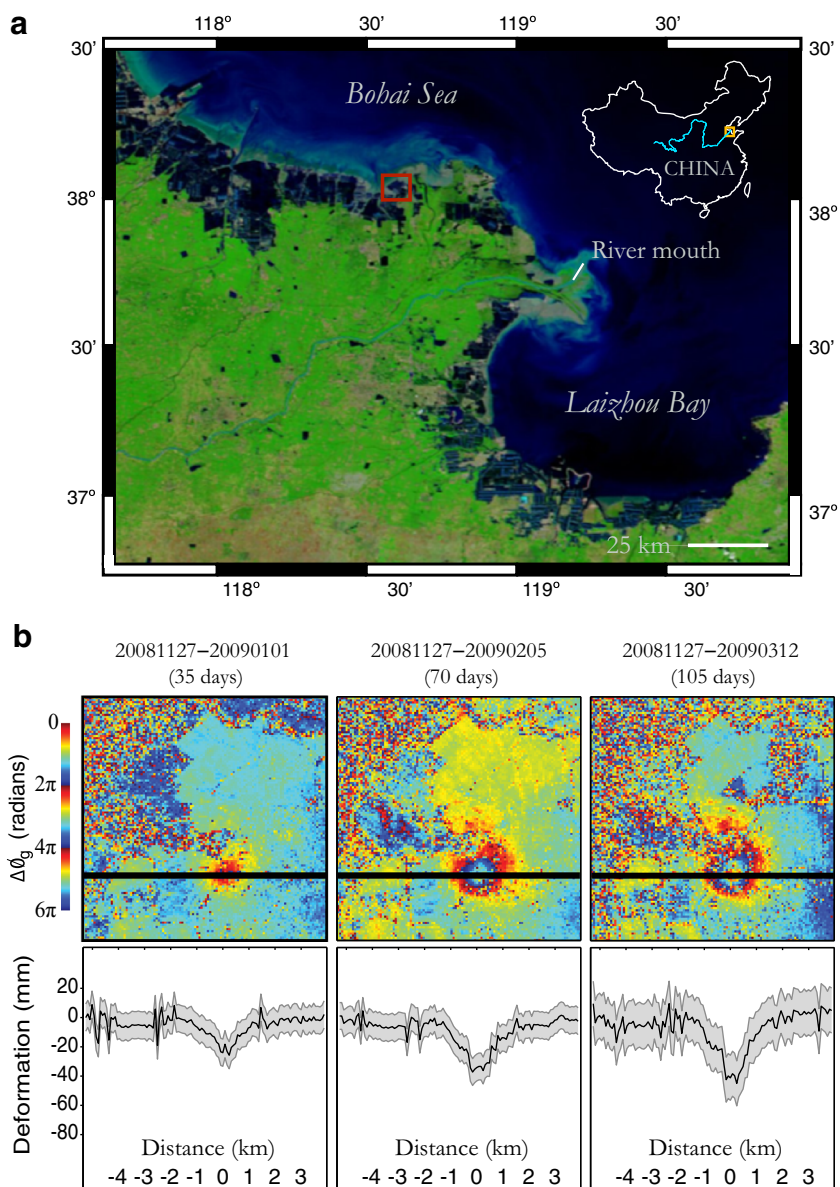
Measuring compaction

An innovative device for measuring natural compaction in wetlands is the Rod Surface Elevation Table (Rod SET), developed by Cahoon et al. (2002). The Rod SET is shown in Fig. 6 and consists of a series of pins attached to a pipe that is anchored at a depth between 1 and 25 m. As the surface subsides, the pins slide downward. Their heights above the reference arm are measured with a ruler at regular intervals to monitor compaction. SETs are often combined with nearby marker horizons to establish the balance between compaction and aggradation.

River deltas are geomorphically complex landforms, however, and natural compaction rates can vary by several orders of magnitude depending on sediment grain size, overburden thickness, and the time since deposition, all of which may vary across a delta at sub-km scales. Given these considerations, mapping techniques such as InSAR and LiDAR are well suited to studying compaction, as they are able to capture spatial variability at a high enough resolution to fully sample the behaviors of a delta's different deposits. They are also useful for distinguishing between natural and anthropogenic compaction on the basis of spatial patterns.

LiDAR (light detection and ranging) is a mapping technique that uses an airborne laser to map surface topography with 15–30 cm accuracy even under thick forest cover

Fig. 5 Higgins et al. (2013)'s InSAR measurements of subsidence due to groundwater extraction at aquaculture facilities in the Yellow River Delta. **a** False-color MODIS image of the Yellow River Delta in September 2012. Water appears dark blue, highlighting the abundance of aquaculture facilities along the coast. Red box corresponds to the InSAR measurements in part **b**. **b** Evolving subsidence bowl at a fish hatchery on the northern shore of the delta. Solid line is cross-section location. Adapted from Higgins et al. (2013) with permission from John Wiley & Sons, Inc



(Reutebuch et al. 2003). LiDAR has been used to map the topography of the Mackenzie Delta (Whalen et al. 2009), the Mississippi River Delta (Cunningham et al. 2004) and the Colorado River Delta (Mueller et al. 2015), though no repeat flights have yet allowed the quantification of subsidence in these deltas. In the United States, LiDAR currently costs on the order of \$40,000.00 to \$100,000.00 to map an area of 1,000 km². Despite the cost, repeat LiDAR has the potential to provide the highest resolution subsidence maps of any available technique.

InSAR is a satellite-based technique that uses phase changes between repeat passes of a synthetic aperture radar (SAR) as a sensitive measure of ground motion towards or away from the satellite. The dominant source of error in deformation measurements comes from atmospheric water vapor, which can cause errors as large as 10–20 cm. However, careful

selection of data acquired on cold, still nights can eliminate these effects (Ferretti et al. 2007). InSAR is capable of producing maps of ground deformation with meter-scale resolution in the horizontal and mm-scale resolution in the vertical (Monti-Guarnieri et al. 1993; Massonnet and Feigl 1998). A limitation of InSAR compared with leveling or LiDAR is that it cannot resolve erosion or aggradation, as it requires ground reflectors to remain precisely the same between successive passes of the satellite. However, InSAR is ideal for measuring compaction that occurs beneath buildings, roads, levees, and even light vegetation.

Perhaps the first study to apply InSAR to a major river delta was Dixon et al. (2006), who measured subsidence rates in New Orleans in the years leading up to Hurricane Katrina (Fig. 7). Subsidence rates over the period 2002–2005 ranged from less than 0 (uplift) to 33 mm/year, with variability of



Fig. 6 The Rod Surface Elevation Table (Rod SET), developed by Cahoon et al. (2002) for measuring surface elevation change in wetlands. The SET is anchored at a depth between 1 and 25 m, and pins rest gently on the wetland surface. As the surface subsides due to natural compaction, the pins slide downward. Their heights above the reference arm are measured with a ruler at regular intervals in order to monitor compaction. SETs are often combined with nearby marker horizons to establish the balance between compaction and aggradation. Photo credit: Donald Cahoon, US Geological Survey, used with permission

more than 20 mm/year occurring over sub-km distances. Subsidence rates were highest along the Mississippi River-Gulf Outlet (MRGO) canal, which breached in multiple places during the storm.

Many studies have since applied InSAR to deltas. Some have found significant relationships between subsidence patterns and underlying stratigraphy. In the Nile Delta, Becker and Sultan (2009) were able to demonstrate that the fastest subsidence rates did not correspond to the thinnest sediments, as Stanley and Warne (1993) proposed, but rather to the youngest sediments. Teatini et al. (2011) examined the Po Delta in Italy, where natural gas production caused as much as 3 m of land subsidence between the 1930s and the 1970s. Today, InSAR shows that subsidence rates are just 1–15 mm/year and are correlated with the age of shallow Holocene deposits, suggesting that

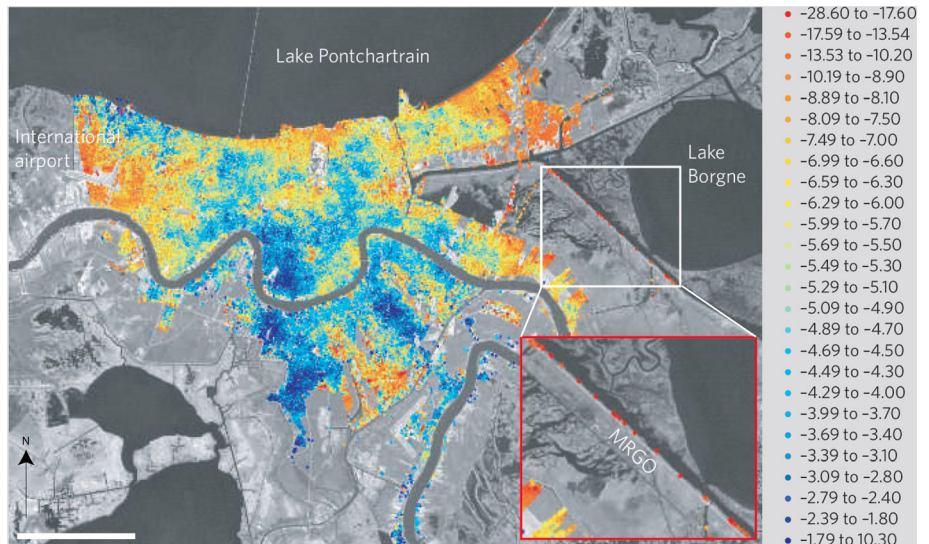
consolidation of these deposits is now the major cause of current land subsidence in the Po Delta (Teatini et al. 2011). Higgins et al. (2014) used InSAR to map natural compaction in the Ganges-Brahmaputra Delta, Bangladesh, where frequent avulsions have created complex subsurface stratigraphy such that surface sediment type does not always reflect subsurface grain size and porosity. Results show variability in subsidence rates of up to one order of magnitude on sub-km scales, correlated with surface and sub-surface sediment type. These findings suggest that, where anthropogenic influences are minimal, mapping subsidence at high spatial resolution with InSAR can reveal subsurface stratigraphy through differences in compaction rates.

A limitation of InSAR is that it cannot measure deformation with a footprint wider than a swath width, 50–300 km for most SAR satellites. InSAR performs best when measuring deformation that ranges from meters to tens of kilometers in its horizontal extent. This limitation is due to slight inaccuracies in satellite orbital knowledge, which produce a linear or quadratic signal across most interferograms (an interferogram is a map of phase change between two SAR scenes). The signal is fitted and removed as a standard step in InSAR processing (Ferretti et al. 2007; Bähr and Hanssen 2012; Fig. 8). This step effectively removes long-wavelength signals as well, filtering out deformation with similar spatial characteristics such as tectonic movement or tides (Bähr and Hanssen 2012). Mosaics of several tracks show a broad area but present only residual motion within tracks that have long-wavelength deformation set to zero. GPS or other measurements are necessary to independently determine longer-wavelength patterns.

Measuring aggradation

Aggradation is a critical piece of the delta balance, as new sediment deposits are the only way to maintain surface elevation despite deeper subsidence. With the exception of repeat

Fig. 7 Dixon et al. (2006)'s measurements of land subsidence in New Orleans, Louisiana (USA). Scale bar is 10 km. Velocity values are mm/year in the line of sight of the radar. Reprinted by permission from Macmillan Publishers Ltd: Nature 441: 587–588, 2006



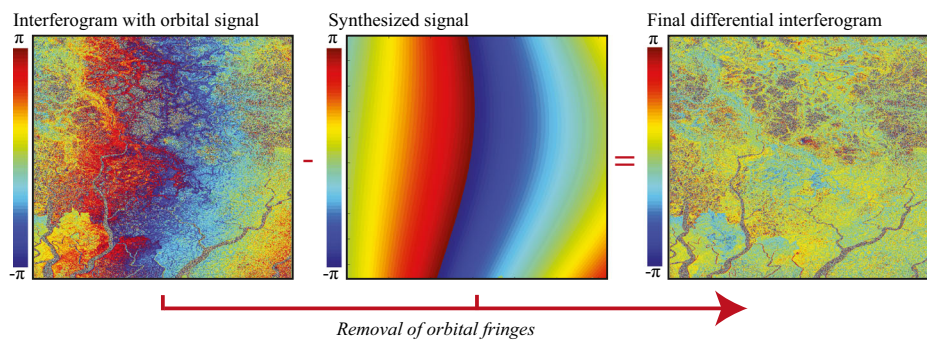


Fig. 8 Example of synthesizing and removing orbital fringes during InSAR processing. Synthesized signal was generated using the Repeat Orbit Interferometry Package (ROI_PAC) ver. 3.0.1 (Rosen et al. 2004). METI (Ministry of Economy, Trade and Industry) and JAXA (Japan

Aerospace Exploration Agency) retain ownership of the original ALOS (Advanced Land Observing Satellite) PALSAR (Phased Array L-band Synthetic Aperture Radar) data, which were distributed by the Alaska Satellite Facility

LiDAR, no airborne or satellite-based method can measure aggradation rates. InSAR is blind to erosion and deposition due to a loss of pixel coherence, while GPS can only detect motion beneath the buildings or platforms upon which the devices sit. Ground-based measurements of aggradation must complement InSAR or GPS where it is possible for sediment deposition to occur.

Short-term aggradation can be measured with marker horizons such as brick dust or powdered feldspar sprinkled on the land surface (e.g., Cahoon et al. 2002; Krauss et al. 2003; Lovelock et al. 2011; Rogers et al. 2013b). Sediment accumulates atop the marker horizon, which is excavated at a later time in order to determine aggradation rates. The marker horizon is an ideal technique for measuring pure aggradation because it is not sensitive to any other component of relative sea-level rise. Horizons tend to degrade quickly, however, and must be refreshed on the order of months (Lovelock et al. 2011).

For longer-term measurements, sediment cores can yield aggradation rates over hundreds or even thousands of years. The contents of a core reflect sediments that have aggraded and peat that has developed and persisted; these strata may also have compacted naturally or under anthropogenic influences, and tectonic or isostatic process may have arbitrarily shifted the elevation of reference points such as the paleosurface. Thus, additional techniques are required to obtain pure aggradation measurements from a sediment core, or studies can make use of assumptions about the initial porosity of sediments (e.g., Shi et al. 2007), the initial dry bulk density of peat (e.g., van Asselen 2010) or the location of the paleosurface (e.g., Tornqvist et al. 2008).

Combining techniques and predicting future surface elevation

Surface elevation change measurements are typically undertaken with the end goal of predicting either elevation or relative sea level at some time in the future. Accurate predictions will require combining multiple methods in order to fully

capture and characterize every component of relative sea-level rise. A tide gauge combined with a Rod SET and a marker horizon, for example, could yield a complete measurement of relative sea level change in a delta wetland. InSAR measurements could identify compaction caused by fluid extraction in an urban setting while a GPS array is used to determine regional basin subsidence. Techniques can also be differenced in order to isolate the contributions from a single subsidence process. Extensometers deployed at different depths can be differenced to isolate compaction in different aquifers or to differentiate between aquifer compaction and peat oxidation (e.g., Rojstaccer et al. 1991). Buildings with foundations at different depths can serve the same purpose when GPS or InSAR readings are taken from their rooftops.

Conclusions

As sea level rises, concern is mounting regarding the impacts of land subsidence in the coastal zone. These impacts can include aquifer salinization, infrastructure damage, increased vulnerability to flooding and storm surges, and permanent inundation of low-lying land. River deltas, with their compressible substrates, low gradients and large populations, are particularly vulnerable.

This article synthesized the state of knowledge regarding delta subsidence research, highlighted knowledge gaps, and suggested research paths towards better understanding of delta subsidence processes. In the last 30 years, InSAR and GPS have expanded understanding of tectonics, isostatic adjustment, flexure, natural compaction, and the rapid subsidence associated with fluid extraction both inside and outside of cities. As LiDAR data becomes more widely available, it will facilitate studies of elevation change in rural and vegetated areas. Future studies using airborne and space-based techniques might aim to increase measurements in rural areas of deltas and to further quantify the spatial and temporal variability of each subsidence process. Numerical modeling studies

might examine sediment deposition during storms and floods, coupling deposition to deep processes or tracking grain size in order to estimate the impacts of changing aggradation patterns on local vegetation.

Natural compaction coupled with reduced aggradation is a common cause of subsidence in river deltas. Where heavy fluid extraction exists, however, it can produce larger subsidence rates than any other known process. Rates of subsidence associated with fluid extraction can outpace global average sea level rise by up to two orders of magnitude, resulting in effective sea level rise that is one-hundred times faster than the global average rate. In deltas with significant fluid extraction, the relevant timescale for decision-making may be decadal rather than generational. Such deltas should be monitored with InSAR, GPS and LiDAR in order to facilitate management decisions. This may require the installation of GPS devices on many additional deltas. Despite a current research focus that prioritizes cities, it will also be necessary to quantify subsidence outside of cities, in the vulnerable rural areas and coastal wetlands that now constitute the primary barrier between land and sea. Ground-based measurements will continue to be necessary as well, as ground-based measurements are the only techniques that can fully resolve the aggradation and vegetation change components of the delta surface elevation balance.

Acknowledgements This work was supported by NASA Land-Cover/Land-Use Change (LCLUC) award “Global-scale assessment of threatened river delta systems,” NSF award 1135427 “Frontiers in Earth-System Dynamics (FESD) Type 1: A Delta Dynamics Collaboratory,” and NSF grant DGE 0707432.

References

- Alber M, Swenson EM, Adamowicz SC, Mendelsohn IA (2008) Salt marsh dieback: an overview of recent events in the US. *Estuar Coast Shelf Sci* 80(1):1–11
- Allen JRL (1990) The formation of coastal peat marshes under an upward tendency of relative sea-level. *J Geol Soc Lond* 147:743–745
- Allen JRL (1999) Geological impacts on coastal wetland landscapes: some general effects of autocompaction in the Holocene of north-western Europe. *The Holocene* 9(1):1–12. doi:[10.1191/095968399674929672](https://doi.org/10.1191/095968399674929672)
- Bähr H, Hanssen RF (2012) Reliable estimation of orbit errors in spaceborne SAR interferometry: the network approach. *J Geod* 86(12):1147–1164. doi:[10.1007/s00190-012-0571-6](https://doi.org/10.1007/s00190-012-0571-6)
- Becker RH, Sultan M (2009) Land subsidence in the Nile Delta: inferences from radar interferometry. *The Holocene* 19(6):949–954
- Bloom AL (1964) Peat accumulation and compaction in a Connecticut Coastal Marsh. *J Sediment Res* 34(3):599–603
- Bondesan M, Simeoni U (1983) Dinamica e analisi morfologica statistica del litorale del delta del Po e alle foci dell’Adige e del Brenta [Dynamics and statistical morphological analysis of the Po Delta coast and the mouths of the Adige and Brenta rivers]. *Mem Soc Geol Ital* 36:1–48
- Cahoon DS, Lynch JC, Perez BC, Segura B, Holland RD, Stelly C, Stephenson G, Hensel P (2002) High-precision measurements of wetland sediment elevation II: the Rod Surface Elevation Table. *J Sediment Res* 72(5):730–733
- Cahoon DS, Hensel P, Rybcyzk J, McKee KL, Proffitt CE, Perez BA (2003) Mass tree mortality leads to mangrove peat collapse at Bay islands, Honduras, after Hurricane Mitch. *J Ecol* 91:1093–1105
- Cahoon DS, Ford MA, Hensel PF (2004) Ecogeomorphology of Spartina patens-dominated tidal marshes: soil organic matter accumulation, marsh elevation dynamics, and disturbance, vol 59. American Geophysical Union, Washington, DC, pp 247–266
- Cahoon DS, Hensel PF, Spencer T, Reed DJ, McKee KL, Saintilan N (2006) Coastal wetland vulnerability to relative sea-level rise: wetland elevation trends and process controls, vol 190, chap 12. In: *Wetlands and natural resource management*. Springer, Heidelberg, Germany, pp 271–292
- Caputo M, Pieri L, Unghendoli M (1970) Geometric investigation of the subsidence in the Po Delta. *Boll Geofis Teor Appl* 14(47):187–207
- Chaussard E, Amelung F, Abidin H, Hong S-H (2013) Sinking cities in Indonesia: ALOS PALSAR detects rapid subsidence due to groundwater and gas extraction. *Remote Sens Environ* 128:150–161. doi:[10.1016/j.rse.2012.10.015](https://doi.org/10.1016/j.rse.2012.10.015)
- Church JA, Clark PU, Cazenave A, Gregory JM, Jevrejeva S, Levermann A, Merrifield MA, Milne GA, Nerem RS, Nunn PD, Payne AJ, Pfeffer WT, Stammer D, Unnikrishnan AS (2013) Sea level change, chap 13. In: *Climate change 2013: the physical science basis—contribution of Working Group I to the Fifth Assessment report of the Intergovernmental Panel on Climate Change*. Cambridge University Press, Cambridge
- CIESIN (Center for International Earth Science Information Network) (2005) Gridded population of the world version 3 (GPWv3). Technical report, CIESIN and SEDAC, New York; CIAT, Palisades, NY. <http://sedac.ciesin.columbia.edu/gpw>. Accessed October 2015
- Coleman JM (1969) Brahmaputra River: channel processes and sedimentation. *Sediment Geol* 3(2/3):129–239
- Corthell EL (1897) The delta of the Mississippi River. *Natl Geogr Mag* 8(13):351–358
- Cunningham R, Gisclair D, Craig J (2004) The Louisiana Statewide LiDAR Project. Louisiana State University, Baton Rouge, Louisiana, p 12
- Day JW, Kemp GP, Reed DJ, Cahoon DR, Boumans RM, Suhayda JM, Gambrell R (2011) Vegetation death and rapid loss of surface elevation in two contrasting Mississippi delta salt marshes: the role of sedimentation, autocompaction and sea-level rise. *Ecol Eng* 37: 229–240. doi:[10.1016/j.ecoleng.2010.11.021](https://doi.org/10.1016/j.ecoleng.2010.11.021)
- Dixon TH, Amelung F, Ferretti A, Novali F, Rocca F, Dokka R, Sella G, Kim S-W, Wdowinski S, Whitman D (2006) Subsidence and flooding in New Orleans. *Nature* 441:587–588. doi:[10.1038/441587a](https://doi.org/10.1038/441587a)
- Dokka RK (2006) Modern-day tectonic subsidence in coastal Louisiana. *Geology* 34:281–284
- Douglas BC (2001) Sea level change in the era of the recording tide gauge. In: Douglas BC, Kearney MS, Leatherman SP (eds) *Sea level rise*. Academic, New York, pp 37–62
- Emery K, Aubrey D (1985) Glacial rebound and relative sea levels in Europe from tide-gauge records. *Tectonophysics* 120(3–4):239–255
- Erban LE, Gorelick SM, Zebker HA (2014) Groundwater extraction, land subsidence and sea-level rise in the Mekong Delta, Vietnam. *Environ Res Lett* 9:084010. doi:[10.1088/1748-9326/9/8/084010](https://doi.org/10.1088/1748-9326/9/8/084010)
- Ericson JP, Vorosmarty CJ, Dingman SL, Ward LG, Meybeck M (2006) Effective sea-level rise and deltas: causes of change and human dimension implications. *Glob Planet Chang* 50:63–82. doi:[10.1016/j.gloplacha.2005.07.004](https://doi.org/10.1016/j.gloplacha.2005.07.004)
- Fan H, Huang H, Zeng T (2006) Impacts of anthropogenic activity on the recent evolution of the Huanghe (Yellow) River delta. *J Coast Res* 22(4):888–929. doi: [10.2112/04-0150](https://doi.org/10.2112/04-0150)
- FAO (2007) The world’s mangroves 1980–2005, Technical report FAO forestry paper 153. Food and Agriculture Organization, Rome
- Ferretti A, Monti-Guarnieri A, Prati C, Rocca F, Lichtenegger J (2007) InSAR principles: guidelines for SAR interferometry processing and

- interpretation. Technical report TM-19, European Space Agency, Noordwijk, The Netherlands
- Freeze RA, Cherry JA (1979) Groundwater. Prentice-Hall, Upper Saddle River, NJ
- Galloway D, Jones DR, Ingebritsen SE (1999) Land subsidence in the United States, part II: drainage of organic soils. US Geol Surv Circ 1182:79–106
- Gambolati G, Putti M, Teatini P, Camporese M, Ferraris S, Gasparetto Stori G, Nicoletti V, Silvestri S, Rizzetto F, Tosi L (2005) Peat land oxidation enhances subsidence in the Venice watershed. *EOS Trans Am Geophys Union* 86(23):217–220. doi:[10.1029/2005EO230001](https://doi.org/10.1029/2005EO230001)
- Gambolati G, Putti M, Teatini P, Gasparetto Stori G (2006) Subsidence due to peat oxidation and its impact on drainage infrastructures in a farmland catchment south of the Venice Lagoon. *Environ Geol* 49: 814–820
- Goodbred SL Jr, Kuehl SA, Steckler MS, Sarker MH (2003) Controls on facies distribution and stratigraphic preservation in the Ganges-Brahmaputra delta sequence. *Sediment Geol* 155(34):301–316
- Herodotus (ca. 440 BC) The histories: Book II, G. Rawlinson, Translator, 8th printing, 1997. Knopf, New York
- Higgins S, Overeem I, Tanaka A, Syvitski JPM (2013) Land subsidence at aquaculture facilities in the Yellow River Delta, China. *Geophys Res Lett* 40(15):3898–3902. doi:[10.1002/grl.50758](https://doi.org/10.1002/grl.50758)
- Higgins S, Overeem I, Steckler MS, Syvitski JPM, Akhter SH (2014) InSAR measurements of compaction and subsidence in the Ganges-Brahmaputra Delta, Bangladesh. *J Geophys Res Earth Surf* 119(8): 1768–1781. doi:[10.1002/2014JF003117](https://doi.org/10.1002/2014JF003117)
- Hoeksema RJ (2007) Three stages in the history of land reclamation in the Netherlands. *Irrig Drain* 56:S113–S126. doi:[10.1002/ird.340](https://doi.org/10.1002/ird.340)
- Hooijer A, Page S, Canadell JG, Silvius M, Kwadijk J, Wösten H, Jauhainen J (2010) Current and future CO₂ emissions from drained peatlands in Southeast Asia. *Biogeosciences* 7:1505–1514. doi:[10.5194/bg-7-1505-2010](https://doi.org/10.5194/bg-7-1505-2010)
- Hutton EWH, Syvitski JPM, Watts AB (2013) Isostatic flexure of a infinite slope due to sea-level rise and fall. *Comput Geosci* 53:58–68
- Ibanez C, Prat N, Canicio A (1996) Changes in the hydrology and sediment transport produced by large dams on the lower Ebro River and its estuary. *Regul Rivers: Res Manage* 12(1):51–62
- Ingebritsen SE, Galloway DL (2014) Coastal subsidence and relative sea level rise. *Environ Res Lett* 9, 091002, 4 pp. doi:[10.1088/1748-9326/9/9/091002](https://doi.org/10.1088/1748-9326/9/9/091002)
- Ingebritsen SE, Ikebara ME (1999) Sacramento-San Joaquin Delta: the sinking heart of the state. In: Galloway D, Jones DR, Ingebritsen SE (eds) Land subsidence in the United States, part II: drainage of organic soils. US Geol Surv Circ 1182:83–94
- Invins ER, Dokka RK, Blom RG (2007) Post-glacial sediment load and subsidence in coastal Louisiana. *Geophys Res Lett* 34, L16303
- Johansson JM, Davis JL, Scherneck H-G, Milne GA, Vermeer M (2002) Continuous GPS measurements of post-glacial adjustment in Fennoscandia, part I: geodetic results. *J Geophys Res* 107:2157–2184
- Jouet G, Hutton EWH, Syvitski JPM, Berne S (2008) Response of the Rhone delta margin to loading and subsidence during the last climactic cycle. *Comput Geosci* 35(10):1338–1357
- Krauss K, Allen JA, Cahoon DR (2003) Differential rates of vertical accretion and elevation change among aerial root types in Micronesian mangrove forests. *Estuar Coast Shelf Sci* 56(2):251–259. doi:[10.1016/S0272-7714\(02\)00184-1](https://doi.org/10.1016/S0272-7714(02)00184-1)
- Liu P, Li Q, Li Z, Hoey T, Liu Y, Wang C (2015) Land subsidence over oil fields in the Yellow River Delta. *Remote Sens* 7:1540–1564. doi:[10.3390/rs70201540](https://doi.org/10.3390/rs70201540)
- Long AJ, Waller MP, Stupples P (2006) Driving mechanisms of coastal change: peat compaction and the destruction of late Holocene coastal wetlands. *Mar Geol* 225:63–84
- Lovelock CE, Bennion V, Grinham A, Cahoon DR (2011) The role of surface and subsurface processes in keeping pace with sea level rise in intertidal wetlands of Moreton Bay, Queensland, Australia. *Ecosystems* 14:745–757
- Massey AC, Paul MA, Gehrels WR, Charman DJ (2006) Autocompaction in Holocene coastal back-barrier sediments from south Devon, southwest England. *Mar Geol* 226:225–241
- Massonnet D, Feigl K (1998) Radar interferometry and its application to changes in the Earth's surface. *Rev Geophys* 36:441–500. doi:[10.1029/97RG03139](https://doi.org/10.1029/97RG03139)
- McCarthy TS, Stanistreet IG, Cairncross B, Ellery WN, Ellery K, Oelofse R, Grobicki TSA (1988) Incremental aggradation on the Okavango Delta-fan, Botswana. *Geomorphology* 1:267–278
- McManus J (2002) Deltaic responses to changes in river regimes. *Mar Chem* 79:155–170
- Meckel TA, ten Brink US, Williams SJ (2006) Current subsidence rates due to compaction of Holocene sediments in southern Louisiana. *Geophys Res Lett* 33, L11403
- Meckel TA, Brink UST, Williams SJ (2007) Sediment compaction rates and subsidence in deltaic plains: numerical constraints and stratigraphic influences. *Basin Res* 19:19–31
- Milne GA, Mitrovica JX (2008) Searching for eustasy in deglacial sea-level histories. *Quat Sci Rev* 27(2526):2292–2302. doi:[10.1016/j.quascirev.2008.08.018](https://doi.org/10.1016/j.quascirev.2008.08.018)
- Milne GA, Gehrels WR, Hughes CW, Tamisiea ME (2009) Identifying the causes of sea-level change. *Nat Geosci* 2:471–478. doi:[10.1038/ngeo544](https://doi.org/10.1038/ngeo544)
- Monti-Guarnieri A, Parizzi F, Pasquali P, Prati C, Rocca F (1993) SAR interferometry experiments with ERS-1. *Geosci Remote Sens Symp* 1993(3):991–993
- Morton RA, Bernier JC (2010) Recent subsidence-rate reductions in the Mississippi Delta and their geological implications. *J Coast Res* 26(3):555–561
- Mueller ER, Schmidt JC, Topping DJ, Grams PE (2015) Geomorphic change in the limnophyte reach of the Colorado River in response to the 2014 delta pulse flow, United States and Mexico. In: Proceedings of the 10th Federal Interagency Sedimentation Conference and the 5th Federal Interagency Hydrologic Modeling Conference, Reno, NV, 19–23 April 2015. http://www.sedhyd.org/2015/openconf/modules/request.php?module=oc_program&action=summary.php&id=136
- Nicholls RJ, Cazenave A (2010) Sea-level rise and its impact on coastal zones. *Science* 328:1517–1520. doi:[10.1126/science.1185782](https://doi.org/10.1126/science.1185782)
- Nutalaya P, Yong RN, Chumnankit T, Buapeng S (1996) Land subsidence in Bangkok during 1978–1988, chap 5. Kluwer, Dordrecht, The Netherlands, pp 105–130
- Ostanciaux E, Husson L, Choblet G, Robin C, Pedoja K (2012) Present-day trends of vertical ground motion along the coast lines. *Earth Sci Rev* 110:74–92
- Peltier WR (1999) Global sea level rise and glacial isostatic adjustment. *Glob Planet Chang* 20:93–123
- Rangin C, Klein M, Roques D, Pichon XL, Trong LV (1995) The Red River fault system in the Tonkin Gulf, Vietnam. *Tectonophysics* 243(34):209–222
- Reutebuch SE, McGaughey RJ, Andersen H-E, Carson WW (2003) Accuracy of a high-resolution LiDAR terrain model under a conifer forest canopy. *Can J Remote Sens* 29(5):527–535
- Rojstaccer SA, Hamon RE, Deverel SJ, Massey CA (1991) Evaluation of selected data to assess the causes of subsidence in the Sacramento-San Joaquin Delta, California. U.S. Geological Survey, Sacramento, p 16
- Rogers KG, Overeem I, Higgins S, Gilligan J, Syvitski JPM (2013a) Farming practices and anthropogenic delta dynamics. In: Proceedings of IAHS-IAPSO-IASPEI Assembly, IAHS Publ. Gothenburg, Sweden, p 133–142
- Rogers KG, Goodbred SL Jr, Mondal DR (2013b) Monsoon sedimentation on the ‘abandoned’ tide-influenced Ganges-Brahmaputra delta plain. *Estuar Coast Shelf Sci* 131:297–309

- Rosen PA, Henley S, Peltzer G, Simons M (2004) Updated repeat orbit interferometry package released. *EOS Trans Am Geophys Soc* 85(5):47
- Sanchez-Arcilla A, Jimenez JA, Valdemoro HI (1998) The Ebro Delta: morphodynamics and vulnerability. *J Coast Res* 14(3):754–772
- Shi C, Zhang D, You L, Li B, Zhang Z, Zhang O (2007) Land subsidence as a result of sediment consolidation in the Yellow River Delta. *J Coast Res* 23(1):173–181. doi:[10.2112/39951.1](https://doi.org/10.2112/39951.1)
- Shi X, Fang R, Wu J, Xu H, Sun Y, Yu J (2012) Sustainable development and utilization of groundwater resources considering land subsidence in Suzhou, China. *Eng Geol* 124:77–89. doi:[10.1016/j.engeo.2011.10.005](https://doi.org/10.1016/j.engeo.2011.10.005)
- Shu L, Finlayson B (1992) Flood management on the lower Yellow River: hydrological and geomorphological perspectives. *Sediment Geol* 85:285–296
- Stanley J-D, Randazzo G (2001) Petrologic database to define the human-reworked, sediment-deficient plain of the Rio Grande delta, Texas. *Environ Geol* 41:37–53. doi:[10.1007/s002540100390](https://doi.org/10.1007/s002540100390)
- Stanley J-D, Warne AG (1993) Nile delta: recent geological evolution and human impact. *Science* 260:628–634
- Stanley J-D, Warne AG (1997) Holocene sea level change and early human utilization of deltas. *GSA Today* 7(12):1–7
- Steckler MS, Nooner SL, Akhter SH, Chowdhury SK, Bettadpur S, Seeber L, Kogan MG (2010) Modeling Earth deformation from monsoonal flooding in Bangladesh using hydrographic, GPS, and Gravity Recovery and Climate Experiment (GRACE) data. *J Geophys Res* 115, B08407. doi:[10.1029/2009JB007018](https://doi.org/10.1029/2009JB007018)
- Syvitski JPM (2008) Deltas at risk. *Sustain Sci* 3:23–32
- Syvitski JPM, Kettner A (2011) Sediment flux and the Anthropocene. *Philos Trans R Soc* 369:957–975. doi:[10.1098/rsta.2010.0329](https://doi.org/10.1098/rsta.2010.0329)
- Syvitski JPM, Saito Y (2007) Morphodynamics of deltas under the influence of humans. *Glob Planet Chang* 57:261–282. doi:[10.1016/j.gloplacha.2006.12.001](https://doi.org/10.1016/j.gloplacha.2006.12.001)
- Syvitski JPM, Kettner AJ, Correggiani A, Nelson BW (2005) Distributary channels and their impact on sediment dispersal. *Mar Geol* 222–223:75–94
- Syvitski JPM, Kettner AJ, Overeem I, Hutton EWH, Hannon MT, Brakenridge GR, Day J, Vorusmarty C, Saito Y, Giosan L, Nicholls RJ (2009) Sinking deltas due to human activities. *Nat Geosci* 2:681–686. doi:[10.1038/ngeo629](https://doi.org/10.1038/ngeo629)
- Teatini P, Tosi L, Strozzi T (2011) Quantitative evidence that compaction of Holocene sediments drives the present land subsidence of the Po Delta, Italy. *J Geophys Res* 116, B08407, pp 957–975. doi:[10.1029/2010JB008122](https://doi.org/10.1029/2010JB008122)
- TeBrake WH (2002) Taming the waterwolf: hydraulic engineering and water management in the Netherlands during the Middle Ages. *Technol Cult* 43(3):475–499. doi:[10.1353/tech.2002.0141](https://doi.org/10.1353/tech.2002.0141)
- Tessler ZD, Vörösmarty CJ, Grossberg M, Gladkova I, Aizenman H, Syvitski JPM, Foufoula-Georgiou E (2015) Profiling risk and sustainability in coastal deltas of the world. *Science* 349(6248): 638–643. doi:[10.1126/science.aab3574](https://doi.org/10.1126/science.aab3574)
- Tornqvist TE, Wallace DJ, Storms JEA, Wallinga J, Van Dam RL, Blaauw M, Derkens MS, Klerks CJW, Meijneken C, Snijders EMA (2008) Mississippi Delta subsidence primarily caused by compaction of Holocene strata. *Nat Geosci* 1:173–176
- van Asselen S (2010) Peat compaction in deltas: implications for Holocene delta evolution, PhD Thesis, Utrecht University, The Netherlands, 180 pp
- van Asselen S, Stouthamer E, van Asch Th WJ (2009) Effects of peat compaction on delta evolution: a review on processes, responses, measuring and modeling. *Earth Sci Rev* 92(1–2):35–51. doi:[10.1016/j.earscirev.2008.11.001](https://doi.org/10.1016/j.earscirev.2008.11.001)
- van Asselen S, Karssenberg D, Stouthamer E (2011) Contribution of peat compaction to relative sea-level rise within Holocene deltas. *Geophys Res Lett* 38, L24401. doi:[10.1029/2011GL04983](https://doi.org/10.1029/2011GL04983)
- Vorusmarty CV, Sahagian D (2000) Anthropogenic disturbance of the terrestrial water cycle. *Bioscience* 50:753–765
- Walling DE, Fang D (2003) Recent trends in the suspended sediment loads of the world's rivers. *Glob Planet Chang* 39:111–126
- Wang H, Bi N, Saito Y, Wang Y, Sun X, Zhang J (2010) Recent changes in sediment delivery by the Huanghe (Yellow River) to the sea: causes and environmental implications in its estuary. *J Hydrol* 391: 302–313. doi:[10.1016/j.marenvres.2008.01.003](https://doi.org/10.1016/j.marenvres.2008.01.003)
- Warren RS, Niering WA (1993) Vegetation change on a northeast tidal marsh: interaction of sea-level rise and marsh accretion. *Ecology* 74(1):96–103
- Whalen D, Forbes DL, Hopkinson C, Lavergne JC, Manson GK, Marsh P, Solomon SM (2009) Topographic LiDAR: providing a new perspective in the Mackenzie Delta. Canadian Remote Sensing Society, Lethbridge, AB, 6 pp
- Wolff WJ (1992) The end of a tradition: 1000 years of embankment and reclamation of wetlands in the Netherlands. *Ambio* 21(4):287–291
- Woodroffe CD, Nicholls RJ, Saito Y, Chen Z, Goodbred SL (2006) Landscape variability and the response of Asian megadeltas to environmental change, chap 10. In: Harvey N (ed) Global change and integrated coastal management: the Asia-Pacific region, coastal systems and continental margins. Springer, Dordrecht, doi:[10.1007/1-4020-3628-0_10](https://doi.org/10.1007/1-4020-3628-0_10), pp 277–314
- Xing F, Kettner AJ, Ashton A, Giosan L, Ibanez C, Kaplan JO (2014) Fluvial response to climate variations and anthropogenic perturbations for the Ebro River, Spain in the last 4000 years. *Sci Total Environ* 473–474:20–31
- Xu Y-S, Shen S-L, Cai Z-Y, Zhou G-Y (2008) The state of land subsidence and prediction approaches due to groundwater withdrawal in China. *Nat Hazards* 45:123–135. doi:[10.1007/s11069-007-9168-4](https://doi.org/10.1007/s11069-007-9168-4)
- Zhang J-Z, jun Guang H, bo Bi H (2015) Land subsidence in the modern Yellow River Delta based on InSAR time series analysis. *Nat Hazards* 75:2385–2397. doi:[10.1007/s11069014-1434-7](https://doi.org/10.1007/s11069014-1434-7)